

Proceedings of the 12th International Conference on
Computational Fluid Dynamics in the Oil & Gas,
Metallurgical and Process Industries

Progress in Applied CFD – CFD2017



SINTEF Proceedings

Editors:

Jan Erik Olsen and Stein Tore Johansen

Progress in Applied CFD – CFD2017

Proceedings of the 12th International Conference on Computational Fluid Dynamics
in the Oil & Gas, Metallurgical and Process Industries

SINTEF Academic Press

SINTEF Proceedings no 2

Editors: Jan Erik Olsen and Stein Tore Johansen

Progress in Applied CFD – CFD2017

Selected papers from 10th International Conference on Computational Fluid Dynamics in the Oil & Gas, Metallurgical and Process Industries

Key words:

CFD, Flow, Modelling

Cover, illustration: Arun Kamath

ISSN 2387-4295 (online)

ISBN 978-82-536-1544-8 (pdf)

© Copyright SINTEF Academic Press 2017

The material in this publication is covered by the provisions of the Norwegian Copyright Act. Without any special agreement with SINTEF Academic Press, any copying and making available of the material is only allowed to the extent that this is permitted by law or allowed through an agreement with Kopinor, the Reproduction Rights Organisation for Norway. Any use contrary to legislation or an agreement may lead to a liability for damages and confiscation, and may be punished by fines or imprisonment

SINTEF Academic Press

Address: Forskningsveien 3 B
 PO Box 124 Blindern
 N-0314 OSLO

Tel: +47 73 59 30 00

Fax: +47 22 96 55 08

www.sintef.no/byggforsk

www.sintefbok.no

SINTEF Proceedings

SINTEF Proceedings is a serial publication for peer-reviewed conference proceedings on a variety of scientific topics.

The processes of peer-reviewing of papers published in SINTEF Proceedings are administered by the conference organizers and proceedings editors. Detailed procedures will vary according to custom and practice in each scientific community.

PREFACE

This book contains all manuscripts approved by the reviewers and the organizing committee of the 12th International Conference on Computational Fluid Dynamics in the Oil & Gas, Metallurgical and Process Industries. The conference was hosted by SINTEF in Trondheim in May/June 2017 and is also known as CFD2017 for short. The conference series was initiated by CSIRO and Phil Schwarz in 1997. So far the conference has been alternating between CSIRO in Melbourne and SINTEF in Trondheim. The conferences focuses on the application of CFD in the oil and gas industries, metal production, mineral processing, power generation, chemicals and other process industries. In addition pragmatic modelling concepts and bio-mechanical applications have become an important part of the conference. The papers in this book demonstrate the current progress in applied CFD.

The conference papers undergo a review process involving two experts. Only papers accepted by the reviewers are included in the proceedings. 108 contributions were presented at the conference together with six keynote presentations. A majority of these contributions are presented by their manuscript in this collection (a few were granted to present without an accompanying manuscript).

The organizing committee would like to thank everyone who has helped with review of manuscripts, all those who helped to promote the conference and all authors who have submitted scientific contributions. We are also grateful for the support from the conference sponsors: ANSYS, SFI Metal Production and NanoSim.

Stein Tore Johansen & Jan Erik Olsen



Organizing committee:

Conference chairman: Prof. Stein Tore Johansen

Conference coordinator: Dr. Jan Erik Olsen

Dr. Bernhard Müller

Dr. Sigrid Karstad Dahl

Dr. Shahriar Amini

Dr. Ernst Meese

Dr. Josip Zoric

Dr. Jannike Solsvik

Dr. Peter Witt

Scientific committee:

Stein Tore Johansen, SINTEF/NTNU

Bernhard Müller, NTNU

Phil Schwarz, CSIRO

Akio Tomiyama, Kobe University

Hans Kuipers, Eindhoven University of Technology

Jinghai Li, Chinese Academy of Science

Markus Braun, Ansys

Simon Lo, CD-adapco

Patrick Segers, Universiteit Gent

Jiyuan Tu, RMIT

Jos Derksen, University of Aberdeen

Dmitry Eskin, Schlumberger-Doll Research

Pär Jönsson, KTH

Stefan Pirker, Johannes Kepler University

Josip Zoric, SINTEF

CONTENTS

PRAGMATIC MODELLING	9
On pragmatism in industrial modeling. Part III: Application to operational drilling	11
CFD modeling of dynamic emulsion stability	23
Modelling of interaction between turbines and terrain wakes using pragmatic approach	29
FLUIDIZED BED	37
Simulation of chemical looping combustion process in a double looping fluidized bed reactor with cu-based oxygen carriers.....	39
Extremely fast simulations of heat transfer in fluidized beds.....	47
Mass transfer phenomena in fluidized beds with horizontally immersed membranes	53
A Two-Fluid model study of hydrogen production via water gas shift in fluidized bed membrane reactors	63
Effect of lift force on dense gas-fluidized beds of non-spherical particles	71
Experimental and numerical investigation of a bubbling dense gas-solid fluidized bed	81
Direct numerical simulation of the effective drag in gas-liquid-solid systems	89
A Lagrangian-Eulerian hybrid model for the simulation of direct reduction of iron ore in fluidized beds.....	97
High temperature fluidization - influence of inter-particle forces on fluidization behavior	107
Verification of filtered two fluid models for reactive gas-solid flows	115
BIOMECHANICS.....	123
A computational framework involving CFD and data mining tools for analyzing disease in carotid artery	125
Investigating the numerical parameter space for a stenosed patient-specific internal carotid artery model.....	133
Velocity profiles in a 2D model of the left ventricular outflow tract, pathological case study using PIV and CFD modeling.....	139
Oscillatory flow and mass transport in a coronary artery.....	147
Patient specific numerical simulation of flow in the human upper airways for assessing the effect of nasal surgery.....	153
CFD simulations of turbulent flow in the human upper airways	163
OIL & GAS APPLICATIONS	169
Estimation of flow rates and parameters in two-phase stratified and slug flow by an ensemble Kalman filter	171
Direct numerical simulation of proppant transport in a narrow channel for hydraulic fracturing application	179
Multiphase direct numerical simulations (DNS) of oil-water flows through homogeneous porous rocks	185
CFD erosion modelling of blind tees	191
Shape factors inclusion in a one-dimensional, transient two-fluid model for stratified and slug flow simulations in pipes	201
Gas-liquid two-phase flow behavior in terrain-inclined pipelines for wet natural gas transportation	207

NUMERICS, METHODS & CODE DEVELOPMENT	213
Innovative computing for industrially-relevant multiphase flows	215
Development of GPU parallel multiphase flow solver for turbulent slurry flows in cyclone.....	223
Immersed boundary method for the compressible Navier–Stokes equations using high order summation-by-parts difference operators	233
Direct numerical simulation of coupled heat and mass transfer in fluid-solid systems	243
A simulation concept for generic simulation of multi-material flow, using staggered Cartesian grids.....	253
A cartesian cut-cell method, based on formal volume averaging of mass, momentum equations.....	265
SOFT: a framework for semantic interoperability of scientific software	273
POPULATION BALANCE	279
Combined multifluid-population balance method for polydisperse multiphase flows	281
A multifluid-PBE model for a slurry bubble column with bubble size dependent velocity, weight fractions and temperature.....	285
CFD simulation of the droplet size distribution of liquid-liquid emulsions in stirred tank reactors	295
Towards a CFD model for boiling flows: validation of QMOM predictions with TOPFLOW experiments	301
Numerical simulations of turbulent liquid-liquid dispersions with quadrature-based moment methods.....	309
Simulation of dispersion of immiscible fluids in a turbulent couette flow	317
Simulation of gas-liquid flows in separators - a Lagrangian approach.....	325
CFD modelling to predict mass transfer in pulsed sieve plate extraction columns	335
BREAKUP & COALESCENCE	343
Experimental and numerical study on single droplet breakage in turbulent flow	345
Improved collision modelling for liquid metal droplets in a copper slag cleaning process	355
Modelling of bubble dynamics in slag during its hot stage engineering.....	365
Controlled coalescence with local front reconstruction method	373
BUBBLY FLOWS	381
Modelling of fluid dynamics, mass transfer and chemical reaction in bubbly flows	383
Stochastic DSMC model for large scale dense bubbly flows.....	391
On the surfacing mechanism of bubble plumes from subsea gas release.....	399
Bubble generated turbulence in two fluid simulation of bubbly flow	405
HEAT TRANSFER	413
CFD-simulation of boiling in a heated pipe including flow pattern transitions using a multi-field concept	415
The pear-shaped fate of an ice melting front	423
Flow dynamics studies for flexible operation of continuous casters (flow flex cc).....	431
An Euler-Euler model for gas-liquid flows in a coil wound heat exchanger.....	441
NON-NEWTONIAN FLOWS.....	449
Viscoelastic flow simulations in disordered porous media	451
Tire rubber extrudate swell simulation and verification with experiments	459
Front-tracking simulations of bubbles rising in non-Newtonian fluids.....	469
A 2D sediment bed morphodynamics model for turbulent, non-Newtonian, particle-loaded flows.....	479

METALLURGICAL APPLICATIONS.....	491
Experimental modelling of metallurgical processes	493
State of the art: macroscopic modelling approaches for the description of multiphysics phenomena within the electroslag remelting process	499
LES-VOF simulation of turbulent interfacial flow in the continuous casting mold	507
CFD-DEM modelling of blast furnace tapping	515
Multiphase flow modelling of furnace tapholes	521
Numerical predictions of the shape and size of the raceway zone in a blast furnace.....	531
Modelling and measurements in the aluminium industry - Where are the obstacles?	541
Modelling of chemical reactions in metallurgical processes.....	549
Using CFD analysis to optimise top submerged lance furnace geometries	555
Numerical analysis of the temperature distribution in a martensic stainless steel strip during hardening.....	565
Validation of a rapid slag viscosity measurement by CFD.....	575
Solidification modeling with user defined function in ANSYS Fluent.....	583
Cleaning of polycyclic aromatic hydrocarbons (PAH) obtained from ferroalloys plant.....	587
Granular flow described by fictitious fluids: a suitable methodology for process simulations	593
A multiscale numerical approach of the dripping slag in the coke bed zone of a pilot scale Si-Mn furnace.....	599
INDUSTRIAL APPLICATIONS	605
Use of CFD as a design tool for a phosphoric acid plant cooling pond	607
Numerical evaluation of co-firing solid recovered fuel with petroleum coke in a cement rotary kiln: Influence of fuel moisture	613
Experimental and CFD investigation of fractal distributor on a novel plate and frame ion-exchanger	621
COMBUSTION	631
CFD modeling of a commercial-size circle-draft biomass gasifier.....	633
Numerical study of coal particle gasification up to Reynolds numbers of 1000.....	641
Modelling combustion of pulverized coal and alternative carbon materials in the blast furnace raceway	647
Combustion chamber scaling for energy recovery from furnace process gas: waste to value	657
PACKED BED.....	665
Comparison of particle-resolved direct numerical simulation and 1D modelling of catalytic reactions in a packed bed	667
Numerical investigation of particle types influence on packed bed adsorber behaviour	675
CFD based study of dense medium drum separation processes	683
A multi-domain 1D particle-reactor model for packed bed reactor applications.....	689
SPECIES TRANSPORT & INTERFACES	699
Modelling and numerical simulation of surface active species transport - reaction in welding processes	701
Multiscale approach to fully resolved boundary layers using adaptive grids.....	709
Implementation, demonstration and validation of a user-defined wall function for direct precipitation fouling in Ansys Fluent.....	717

FREE SURFACE FLOW & WAVES	727
Unresolved CFD-DEM in environmental engineering: submarine slope stability and other applications.....	729
Influence of the upstream cylinder and wave breaking point on the breaking wave forces on the downstream cylinder	735
Recent developments for the computation of the necessary submergence of pump intakes with free surfaces	743
Parallel multiphase flow software for solving the Navier-Stokes equations	752
 PARTICLE METHODS	 759
A numerical approach to model aggregate restructuring in shear flow using DEM in Lattice-Boltzmann simulations	761
Adaptive coarse-graining for large-scale DEM simulations.....	773
Novel efficient hybrid-DEM collision integration scheme.....	779
Implementing the kinetic theory of granular flows into the Lagrangian dense discrete phase model.....	785
Importance of the different fluid forces on particle dispersion in fluid phase resonance mixers	791
Large scale modelling of bubble formation and growth in a supersaturated liquid.....	798
 FUNDAMENTAL FLUID DYNAMICS	 807
Flow past a yawed cylinder of finite length using a fictitious domain method	809
A numerical evaluation of the effect of the electro-magnetic force on bubble flow in aluminium smelting process.....	819
A DNS study of droplet spreading and penetration on a porous medium.....	825
From linear to nonlinear: Transient growth in confined magnetohydrodynamic flows.....	831

GAS-LIQUID TWO-PHASE FLOW BEHAVIOR IN TERRAIN-INCLINED PIPELINES FOR WET NATURAL GAS TRANSPORTATION

Yan Yang¹, Jingbo Li¹, Shuli Wang¹, Chuang Wen^{2*}

¹ School of Petroleum Engineering, Changzhou University 213016 Changzhou, CHINA

² Department of Mechanical Engineering, Technical University of Denmark, 2800 Kgs. Lyngby, DENMARK

* E-mail: cwen@mek.dtu.dk

ABSTRACT

The liquid slug formation in a hilly-terrain pipeline is simulated using the Volume of Fluid model and RNG k- ϵ turbulence model. The numerical model is validated by the experimental data of the horizontal slug flow. The influence of pipe diameter on liquid slug formation is discussed in detail. The results show that the pipe is blocked by the liquid slug at the moment of slug formed. The pipe pressure suddenly increases, and then decreases gradually in the process of liquid slug formation and motion. The pipe diameter has little effect on liquid slug formation, while the pipe pressure drop and liquid holdup change small.

Keywords: gas-liquid two-phase flow, CFD, natural gas, pipe flow.

NOMENCLATURE

A complete list of symbols used, with dimensions, is required.

Greek Symbols

α	Volume fraction, [-].
α_k	Constant, [-].
α_ϵ	Constant, [-].
β	Constant, [-].
ϵ	Turbulent dissipation rate, [-].
δ_{ij}	Kronecker delta, [-].
μ	Dynamic viscosity, [m^2s^{-1}].
μ_t	Turbulent viscosity, [m^2s^{-1}].
η_0	Constant, [-].
ρ	Density, [kgm^{-3}].
θ	Inclination angle of pipe, [$^\circ$].
θ_1	Inclination angle of descending pipe, [$^\circ$].
θ_2	Inclination angle of ascending pipe, [$^\circ$].

Latin Symbols

$C_{1\epsilon}$	Constant, [-].
$C_{1\epsilon}^*$	Constant, [-].
$C_{2\epsilon}$	Constant, [-].
C_μ	Constant, [-].
D	Pipe diameter, [mm].
E_{ij}	Mean strain rate, [-].

\vec{F}	External body force, [N].
F_{vol}	Surface force, [N].
G_k	Generation of turbulence kinetic energy, [-].
g	Acceleration of gravity, [m/s^2].
h	Level of stagnant liquid, [mm].
k	Turbulent kinetic energy, [m^2s^{-2}].
L	Pipeline length [m].
\dot{m}_{pq}	Mass transfer from phase p to phase q , [kgs^{-1}].
\dot{m}_{qp}	Mass transfer from phase q to phase p , [kgs^{-1}].
p	Pressure, [Pa].
Q	Volume of pipe, [m^3s^{-1}].
Q_L	Volume of stagnant liquid, [m^3s^{-1}].
S_{aq}	Source term, [-].
t	Time, [s].
u	Velocity, [ms^{-1}].
V_G	Inlet gas velocity [ms^{-1}].
V_{SL}	Superficial liquid velocity [ms^{-1}].
V_{SG}	Superficial gas velocity [ms^{-1}].

Sub/superscripts

G	Gas.
L	Liquid.
i	Index i .
j	Index j .

INTRODUCTION

Natural gas field usually locates in hilly or basin region, and then the hilly-terrain pipelines are used inevitably. The water in wet gas can assemble in the low-lying pipes, and becomes stagnant liquid in the process of transporting wet gas. It leads to the formation of the liquid slug or the slug flow which can cause the shapely pressure and liquid holdup fluctuation in the pipeline. Therefore, it is important to study and predict the slug flow in the hilly-terrain pipelines.

For the slug flow, the study mainly focuses on the horizontal pipe, vertical pipe and hilly-terrain pipes. For the horizontal pipelines, a prediction method based on one-dimensional two-fluid model was presented for

predicting hydrodynamic slug initiation and growth by Issa and Kempf (2003). Al-Safran et al. (2015) proposed a new empirical relationship for predicting slug liquid holdup in high viscosity liquids. For the studies of a slug in the vertical pipelines, Taha and Cui (2006) used the Volume of Fluid (VOF) model to simulate the motion of a single Taylor bubble in the vertical tubes and obtained the shape and flow parameters of the slug. Abdulkadir et al. (2015) conducted the experimental and numerical studies in the vertical pipes with 6 m long and 0.067 m internal diameter. Henau and Raithby (1995) investigated the slug behavior in two-phase pipes which contained several uphill and downhill sections. Ersoy et al. (2011) investigated gas-oil-water three-phase slug flow in hilly-terrain pipelines.

The gas-liquid slug flow attracts attention all the time. However, the formation and motion of a single liquid slug still needs to be further studied in hilly-terrain pipelines, in particular the existence of the stagnant liquids. In this paper, the numerical study is carried out to understand the formation process of a single liquid slug in hilly-terrain pipelines. The influence of pipe diameter on liquid slug formation is analysed in detail.

MODEL DESCRIPTION

The slug flow is a sort of complex gas-liquid flow which has a distinct phase interface. The interface catching is a key step for the simulation of the liquid slug. The Volume of Fluid (VOF) model is a kind of surface-tracking technology based on fixed Eulerian mesh and it can be used for modelling two or more immiscible fluids. Therefore, the VOF model is employed here to track the gas-liquid phase interface in hilly-terrain pipelines. In addition, the turbulence model is necessary due to the flow is turbulent in our simulation.

Governing Equation

Continuity equation

$$\frac{\partial \rho}{\partial t} + \frac{\partial}{\partial x_i} (\rho u_i) = 0 \quad (1)$$

Momentum equation

$$\begin{aligned} \frac{\partial}{\partial t} (\rho \vec{u}) + \nabla \cdot (\rho \vec{u} \vec{u}) \\ = -\nabla p + \nabla \cdot \left[\mu (\nabla \vec{u} + \nabla \vec{u}^T) \right] + \rho \vec{g} + \vec{F} \end{aligned} \quad (2)$$

where ρ is the density, \vec{u} is the velocity, p is the static pressure, μ is the dynamic viscosity, \vec{g} is the gravitational acceleration and \vec{F} is external body force.

Volume fraction equation

$$\frac{1}{\rho_q} \left[\frac{\partial}{\partial t} (a_q \rho_q) + \nabla \cdot (a_q \rho_q \vec{v}_q) \right] = S_{a_q} + \sum_{p=1}^n (\dot{m}_{pq} - \dot{m}_{qp}) \quad (3)$$

where \dot{m}_{pq} is the mass transfer from phase q to phase p and \dot{m}_{qp} is the mass transfer from phase p to phase q ,

α_q is the volume fraction of phase q , S_{α_q} is the source term.

Continuum Surface Force Model

The effect of surface force along the interface is included in the VOF model. The continuum surface force (CSF) model proposed by Brackbill et al (1992) is used in this paper. It is implemented as a source term in the momentum equation. The surface force F_{vol} is expressed as follows:

$$F_{vol} = \sigma_{ij} \frac{\rho \kappa_i \nabla \alpha_i}{\frac{1}{2} (\rho_i + \rho_j)} \quad (4)$$

where

$$\rho = \alpha_2 \rho_2 + (1 - \alpha_2) \rho_1 \quad (5)$$

$$\kappa = \nabla \cdot \hat{n} \quad (6)$$

$$\hat{n} = \frac{n}{|n|} \quad (7)$$

$$n = \nabla \alpha_q \quad (8)$$

Turbulence Model

The RNG k - ε turbulence model has an additional term in its ε equation that significantly improves the accuracy for rapidly strained flows. It also provides an option to account for the effects of swirl or rotation by modifying the turbulent viscosity appropriately. Therefore, the RNG k - ε turbulence model is employed here because the flow turns at the elbow of the pipe which connects the uphill section and downhill section in hilly-terrain pipelines. The turbulence kinetic energy, k , and its rate of dissipation, ε , are as follows:

$$\begin{aligned} \frac{\partial(\rho k)}{\partial t} + \frac{\partial(\rho k u_i)}{\partial x_i} \\ = \frac{\partial}{\partial x_j} \left[\alpha_k \mu_{eff} \frac{\partial k}{\partial x_j} \right] + G_k + \rho \varepsilon \end{aligned} \quad (9)$$

$$\begin{aligned} \frac{\partial(\rho \varepsilon)}{\partial t} + \frac{\partial(\rho \varepsilon u_i)}{\partial x_i} \\ = \frac{\partial}{\partial x_j} \left[\alpha_\varepsilon \mu_{eff} \frac{\partial \varepsilon}{\partial x_j} \right] + \frac{C_{1\varepsilon}^* \varepsilon}{k} G_k - C_{2\varepsilon} \rho \frac{\varepsilon^2}{k} \end{aligned} \quad (10)$$

where

$$\mu_{eff} = \mu + \mu_t \quad (11)$$

$$\mu_t = \rho C_\mu \frac{k^2}{\varepsilon} \quad (12)$$

$$C_{1\varepsilon}^* = C_{1\varepsilon} - \frac{\eta(1 - \eta / \eta_0)}{1 + \beta \eta^3} \quad (13)$$

$$\eta = (2E_{ij} \cdot E_{ij})^{1/2} \frac{k}{\varepsilon} \quad (14)$$

$$E_{ij} = \frac{1}{2} \left(\frac{\partial u_i}{\partial x_j} + \frac{\partial u_j}{\partial x_i} \right) \quad (15)$$

where $C_\mu=0.0845$, $\alpha_k=\alpha_\varepsilon=1.39$, $C_{1\varepsilon}=1.42$, $C_{2\varepsilon}=1.68$, $\eta_0=4.377$, $\beta=0.012$.

GEOMETRY AND MESH

The sketch of hilly-terrain pipeline is shown in Figure 1. This pipeline contains a descending pipe and an ascending pipe, respectively. The inclination angles of two pipes are θ_1 and θ_2 . The stagnant liquid is water and the gas phase is methane. Two pressure monitoring points (P1 and P2) are set at the center of the pipe cross section which locates in $x = -15 D$ and $x = 15 D$. The pipe pressure drop is the value of $|P1 - P2|$ in this paper.

The computational domain should be meshed after the geometric model is established. The commercial software ANSYS ICEM CFD is selected as the meshing tool. The hexahedral mesh and O-block technology are selected as the grid partition strategy for improving the quality of grid. The grid system is shown in Figure 2. Around 300 000 cells are performed for our simulations after the grid independence test.

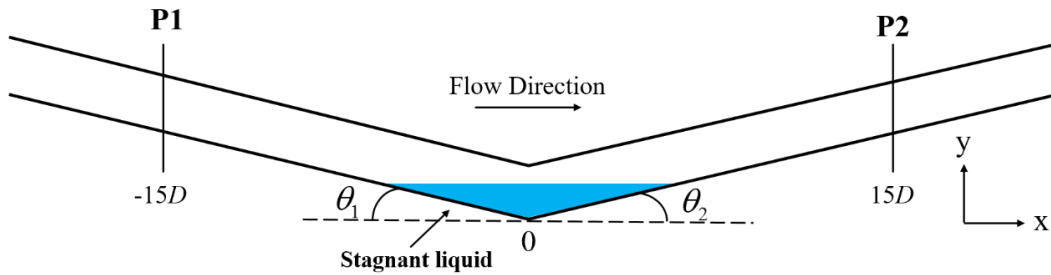


Figure 1 Sketch of the hilly-terrain pipeline

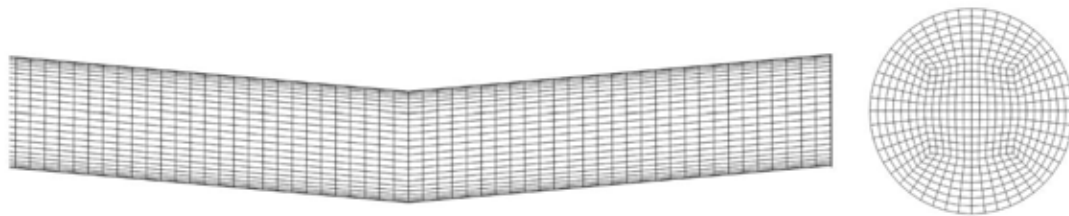


Figure 2 Mesh generation

RESULTS AND DISCUSSION

Model Validation

In this paper the experimental data obtained by Heywood and Richardson (1979) are employed to validate our numerical method. The experiments were carried out in an air-water flow loop system, which included a horizontal pipeline of 42 mm inner diameter. The γ -ray absorption method was used to measure the slug liquid holdup (liquid volume fraction). Six experimental data in the same superficial liquid velocity (0.978 m/s) were selected for the model validation in different superficial gas velocities. The results of the comparison between the experimental and numerical data are shown in Figure 3. It presents that the maximum relative error is 5.9% in superficial gas velocity of 4.145 m/s. Therefore, the numerical results are in good agreement with the experimental data.

x is the position coordinates of pipe along the flow direction.

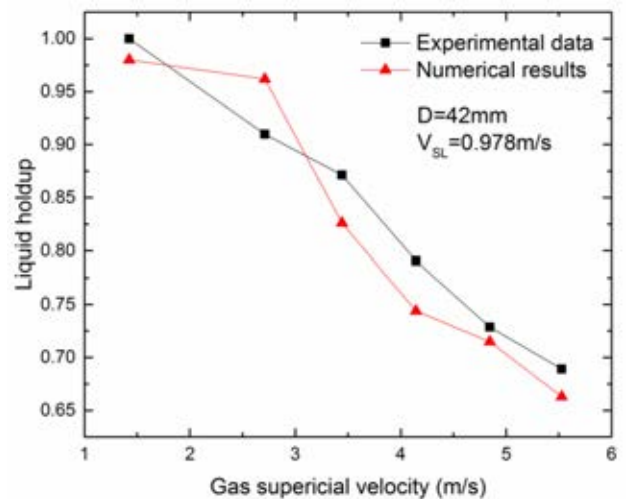


Figure 3 Comparison between experimental and numerical results in a horizontal pipe

Liquid Slug Formation Process

Figure 4 shows the formation process of a liquid slug in the 150 mm diameter pipe with the inclination angle of $\theta_2 = \theta_2 = 5^\circ$. The inlet gas velocity is 6.5 m/s, and the ratio of the stagnant liquid height, h , to the pipe diameter is 0.75 ($h/D=0.75$). The phase fraction distribution with different moment (t) is described in the contours. The blue region represents the gas phase, while the red one represents the liquid phase. The axis,

The flow area decreases due to the stagnant liquid accumulated at the bottom of hilly-terrain pipes, which cause the increase of the gas velocity. This flow structure further induces the decline of the pressure above the liquid level. Then suction force generates in the vertical upward, which destroys the stability of gas-liquid interface. For this reason, a wave crest forms. When the liquid level uplifts to the top of the pipe and

blocks the entire pipe cross section, the liquid slug flow finally appears ($t=0.005$ s -0.100 s in Figure 4). The liquid slug then goes into the next process of moving

forward under the pressure difference between the upstream and downstream of the slug flow ($t=0.105$ -0.120 s in Figure 4).

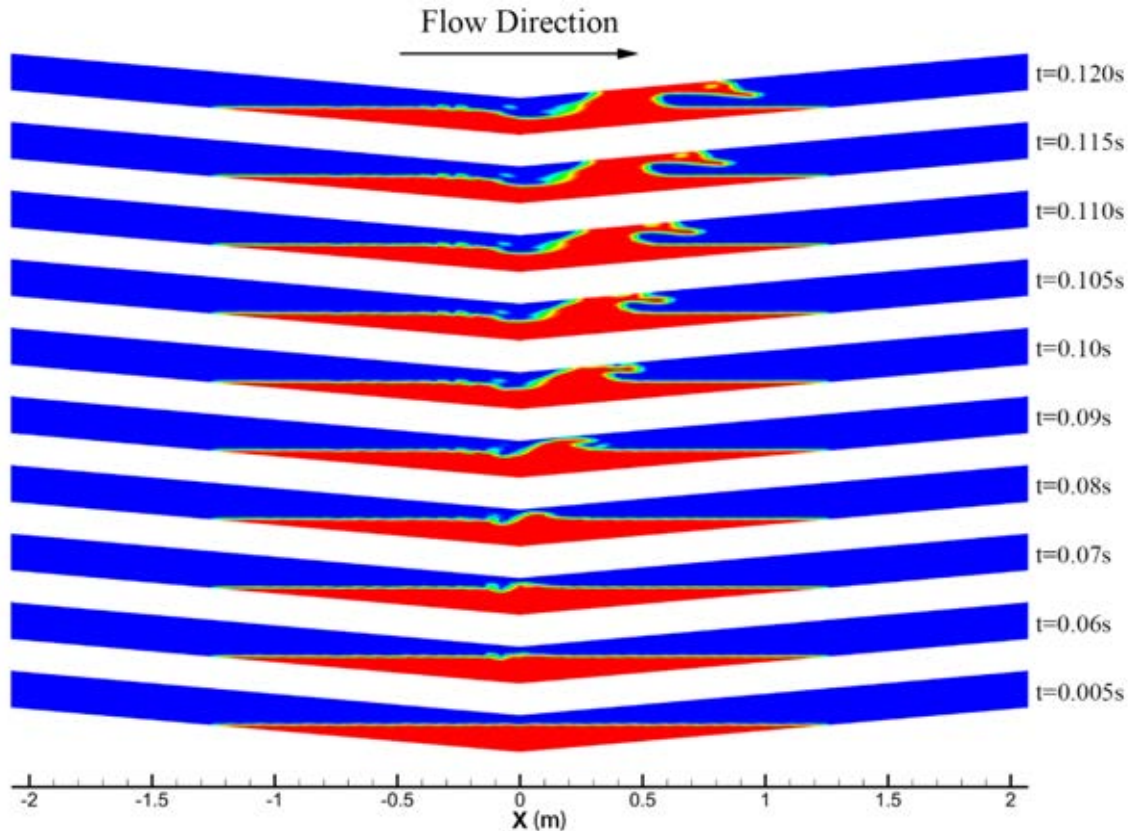


Figure 4 Formation process of a liquid slug

Pipe Diameter Effect

In this section, the influence of the pipe diameter on the formation of a liquid slug is discussed in detail. The pipe diameters are 90 mm, 120 mm, 150 mm, 180 mm and 210 mm, respectively. The length of the ascending and descending pipes is $50 D$, while the inclination angle is set to be 5° . The numerical simulation is implemented in the identical condition which the inlet gas velocity is 6.5 m/s with $h/D=0.75$.

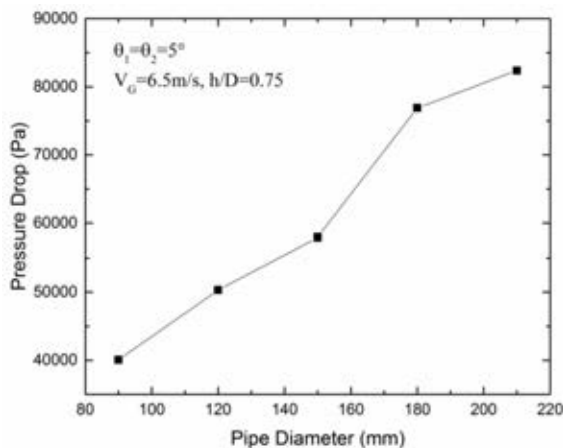


Figure 5 Influence of pipe diameter on pressure drop at the moment of slug formed

The pressure drops in different pipe diameter at the moment of slug formed are shown in Figure 5. The pressure drop increases along with the pipe diameter.

The pressure drop ranges from 40,000 Pa to 82,000 Pa. The rate of increasing pressure drop is about 30% with the pipe diameter from 90 mm to 210 mm. Figure 6 describes the slug liquid holdup in different pipe diameters. We can see that the liquid holdup increases slowly in the pipe diameters from 90 mm to 180 mm, while it declines slightly in the 210 mm diameter pipe. However, the value of slug liquid holdup distributes approximately 0.5 in the entire pipe diameters.

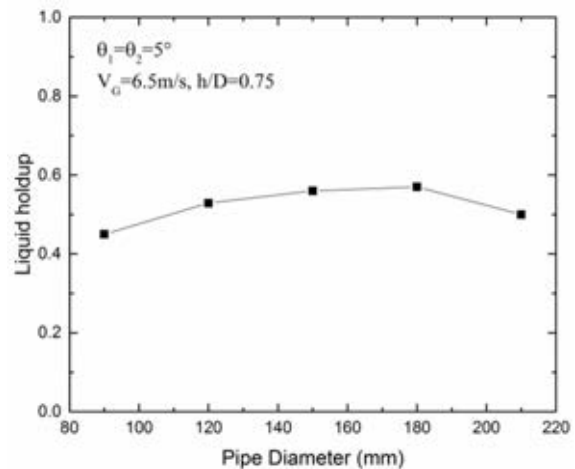


Figure 6 Influence of pipe diameter on liquid holdup at the moment of slug formed

CONCLUSIONS

The VOF and RNG $k-\epsilon$ turbulence models show the reasonable results in simulating the formation process

of a liquid slug. The distinct gas-liquid two-phase distribution and the formation process of a liquid slug are obtained by numerical simulation. The pipe cross-section is blocked by the liquid phase at the moment of a liquid slug formed. The pressure suddenly increases, and then declines gradually in process of liquid slug formation and motion. The pipe diameter has tiny effect on the slug formation, since the pressure drop and the liquid holdup change little.

ACKNOWLEDGEMENTS

This work was supported by the National Natural Science Foundation of China (51444005, 51574045).

REFERENCES

- ABDULKADIR, M., HERNANDEZ-PEREZ, V., LO, S., LOWNDES, I.S. and AZZOPARDI, B.J., (2015), "Comparison of experimental and Computational Fluid Dynamics (CFD) studies of slug flow in a vertical riser", *Exp. Therm Fluid Sci.*, **68**, 468-483.
- AL-SAFRAN, E., KORA, C. and SARICA, C., (2015), "Prediction of slug liquid holdup in high viscosity liquid and gas two-phase flow in horizontal pipes", *J. Pet. Sci. Technol.*, **133**, 566-575.
- BRACKBILL, J.U., KOTHE, D.B. and ZEMACH, C., (1992), "A continuum method for modeling surface tension", *J. Comput. Phys.*, **100**, pp.335-354.
- CLARKE, A. and ISSA, R.I., (1997), "A numerical model of slug flow in vertical tubes", *Comput. Fluids*, **26**, 395-415.
- ERSOY, G., SARICA, C., AL-SAFRAN, E. and ZHANG, H.Q., (2011), "Experimental Investigation of Three-Phase Gas-Oil-Water Slug Flow Evolution in Hilly-Terrain Pipelines", *SPE Annual Technical Conference and Exhibition*, Denver, Colorado, USA, 30 October - 2 November.
- DE HENAU, V. and RAITHBY, G.D., (1995), "A study of terrain-induced slugging in two-phase flow pipelines", *Int. J. Multiphase Flow*, **21**, 365-379.
- HEYWOOD, N.I. and RICHARDSON, J.F., (1979), "Slug flow of air—water mixtures in a horizontal pipe: Determination of liquid holdup by γ -ray absorption", *Chem. Eng. Sci.*, **34**, 17-30.
- ISSA, R.I. and KEMPF, M.H.W., (2003), "Simulation of slug flow in horizontal and nearly horizontal pipes with the two-fluid model", *Int. J. Multiphase Flow*, **29**, 69-95.
- TAHA, T. and CUI, Z.F., (2006), "CFD modelling of slug flow in vertical tubes", *Chem. Eng. Sci.*, **61**, 676-687.